Carbon Budget Concept and its Deviation Through the Pulse Response Lens

Vito Avakumović [1]

[1]Center for Earth System Research and Sustainability (CEN), University of Hamburg, Grindelberg 5, 20144 Hamburg, Germany

Correspondence: Vito Avakumović (vito.avakumovic@uni-hamburg.de)

Abstract. The carbon budget concept states that the global mean temperature (GMT) increase is roughly linearly dependent on cumulative emissions of CO_2. The proportionality is measured as the transient climate response to cumulative emissions of carbon dioxide (TCRE). In this paper, the deviations of the carbon budget from the strict linear relationship implied by the TCRE is examined through the lens of a temperature response to an emission pulse (i.e., pulse response), and its relationship with a non-linear TCRE. Hereby, two sources of deviation are distinguished: emission scenario and climate state-dependence. The former stems from the scenario choice, i.e. the specific emission pathway for a given level of cumulative emissions, and the latter from the change in TCRE with changing climatic conditions. Previous literature argues for scenario independence using a stylized set of emission scenarios, and offers a way to fit a non-linear carbon budget equation. This paper shows how the pulse response, viewed as a Green's function, gives a unifying perspective on both scenario and state-dependence. Moreover, it provides an optimisation program that tests the scenario independence under the full range of emission pathways for a given set of constraints. In a setup chosen in this paper, the deviations stemming from emission pathway choices are less than 10% of the overall temperature increase and gradually diminish. Moreover, using the pulse response as a Green's function, the scenario-dependent effects of a reduced-complexity climate model were replicated to a high degree, confirming that the behaviour of scenario-dependent deviations can be explained and predicted by the shape of the pulse response. Additionally, it is shown that the pulse response changes with climatic conditions, through which the carbon budget state-dependency is explained. Using a pulse response as an approximation for a state-dependent TCRE, an alternative method to derive a non-linear carbon budget equation is provided. Finally, it is shown how different calibrations of a model can lead to different degrees of carbon budget non-linearities. The analysis is done using FaIRv2.0.0, a simple climate emulator model that includes climate feedback modifying the carbon cycle, along with a one-box model used for comparison purposes. The Green's function approach can be used to diagnose both models' carbon budget scenario-dependency, paving the way for future investigations and applications with other and more complex models.

1 Introduction

The carbon budget concept, or the carbon budget approach, has gained prominence over the last decade due to its ability to determine allowable carbon dioxide emissions leading to a specific global mean temperature (GMT) increase. In essence, it

assumes a direct link between the total cumulative carbon emissions and the temperature increase without the need to know the preceding emission pathway. Following the concurrent initial discoveries in the late 2000s (Allen et al. (2009), Matthews et al. (2009), Meinshausen et al. (2009), Zickfeld et al. (2009)), the concept received wider recognition after being included in the IPCC AR5 WG1 [1] (Stocker et al., 2013), and after being presented as an explicit policy recommendation tool for limiting future climate change in IPCC AR6 WG1 (Table SPM.2) (Masson-Delmotte et al., 2021), where the 'remaining carbon budgets' indicate how much carbon may be emitted while still reaching low-temperature targets, assuming net-zero emissions afterward. By and large, since its emergence, the carbon budget has become 'a staple of climate policy discourse', having paved the way for various discourses, from policy proposals and international climate justice discussions to financial recommendations and even climate activism arguments for the immediate abandonment of fossil fuels, to name a few (Lahn, 2020).

Formally, the carbon budget assumes the GMT increases nearly linearly with cumulative emissions, regardless of the preceding carbon emission scenario. Hence, a linear carbon budget equation:

$$T(t) = \Lambda F(t), \tag{1}$$

where $F(t) = \int_0^t E(\tau)\mathrm{d}\tau$ stands for cumulative emissions, and Λ is the proportionality constant, called the transient climate response to cumulative CO_2 emissions (TCRE). The (nearly) linear relationship emerges due to non-linearities cancelling each other out: a concave temperature dependency on the atmospheric carbon content and a convex atmospheric CO_2 dependency on cumulative emissions (Matthews et al. (2009), Raupach (2013)). The former stems from the radiative efficiency saturation of the atmospheric carbon, the latter from the declining ocean heat uptake and the weakening of natural carbon sinks (MacDougall and Friedlingstein, 2015).

When it comes to explicitly determining the remaining budget to reach a certain temperature target, a segmented framework had been devised by Rogelj et al. (2018). In essence, it determines what amount of cumulative emissions will lead to a given level of peak warming, if historical, non-CO_2 and Zero Emission Commitment (ZEC) warming are subtracted. ZEC is another metric closely related to TCRE and measures the warming (or cooling) that occurs after emission cessation (Matthews and Weaver, 2010). MacDougall et al. (2020) show that different models perform differently, with an inter-model range of ZEC 50 years following the emission cessation being -0.36 to 0.29 K. If ZEC were 0, then there would be no time delay in temperature response, and emissions would directly map to temperature according to TCRE. In reality, there is always some time lag between the input and the climate system's response (e.g., Ricke and Caldeira (2014)). Regardless of ZEC, the linear segmented framework concept itself has been revisited by Nicholls et al. (2020), who show that its assumption of a linear relationship between peak warming and cumulative emissions leads to lower budgets, albeit this effect is small in context of other uncertainties.

Hence, there is evidence that the relationship between the temperature and cumulative emissions (Eq. (1)) can be non-linear, as either of the two (convex or concave) mechanisms mentioned above could hypothetically outweigh the other under higher climatic stress (higher T). Indeed, Gillett et al. (2013) show that the linear relationship overestimates temperature response in

---

[1]It was not labeled explicitly as a budget but rather presented implicitly through the emphasis on temperature dependency on cumulative emissions (see Figure AR5 SPM.10).

most Earth System Models (ESMs). Using the FaIR simple climate model (SCM), Leach et al. (2021) quantify the TCRE drop to approximately 10% per 1000 PgC. Additionally, Leduc et al. (2015) have shown that constant TCRE is a good approximation for temperature response under low-emission scenarios, while it overestimates the model's response to high-intensity scenarios;

60 this reaffirms the need for TCRE to decrease in order for the relationship in Eq. (1) to hold true. In the extant literature, Nicholls et al. (2020) have derived the non-linear carbon budget equation by positing a logarithmic relationship between cumulative emissions and temperature increase with a multiplying factor that allows the relationship to be both convex and concave. In this paper, the change in TCRE with changing climatic conditions is referred to as (climate) *state-dependent carbon budget deviation*.

65 Further on, an alternative source of deviation from the budget approach that stems only from the choice of emission scenario, and not from the initial and final climate conditions of the system, is possible. In this paper, this type of deviation is referred to as an *emission scenario-dependent carbon budget deviation*. Previous literature, utilizing high-complexity climate models (ESMs), tends to argue in favour of scenario independence (Gillett et al., 2013). However, the problem with using ESMs to study the emission scenario effects is that these models are very costly from a computational standpoint, which means only a

70 limited set of emission pathways are examined. Using a climate model of intermediate complexity, Herrington and Zickfeld (2014) tested the robustness of the scenario independence with a set of 24 emission scenarios. Millar et al. (2016) addressed this problem by forcing the simplified, globally aggregated climate model under various emission scenarios. However, to the best of the author's knowledge at the time of writing, the entire portfolio of emission scenarios that would yield the extreme cases of maximum possible scenario-dependent carbon budget deviations has yet to be investigated and scrutinized.

75 There is evidence that state- and scenario-dependent deviations are conditional on the model's complexity (MacDougall, 2017), suggesting that models with low linearity have a higher path dependence and vice versa. In this paper, the two effects are approached as separate entities, as the emission scenario-dependent carbon budget deviation implies the possibility of achieving a different temperature T by following a different emission pathway with the same total cumulative emissions F. On the other hand, it is exactly the change in F (and consequently T) that drives the state-dependency of TCRE. As will be shown

80 in this paper, with conclusions restricted to the model inspected, one can have one without the other, with the conditions given explicitly.

At its core, this study is focused on conducting a thorough assessment of deviations within the carbon budget approach, encompassing both scenario- and state-dependent deviations. The study introduces a novel concept termed the "pulse response representation", referring to the analysis of a temperature response to an emission pulse, under different climatic conditions.

85 This conceptual framework proves to be a convenient and effective tool for explaining the observed deviations.

A reinterpretation of the carbon budget equation is suggested using a pulse response in the context of Green's function equation. It is shown that the linear carbon budget equation is only a special case of the Green's function equation. More importantly, the paper demonstrates that, by utilizing the pulse response as a Green's function, one can capture scenario-dependent deviation effects. Hence, it is revealed that, merely by assessing the shape of the pulse response, one can directly

90 deduce to which extent the model adheres to carbon budget scenario independence.

The Green's function's validity is assessed through an optimization program functioning as the generator of scenario-dependent deviations. Specifically, the optimization program empowers users to assess the entire portfolio of emission scenarios, generating extreme cases of maximum scenario-dependent deviations within user-defined constraints. As such, the optimization program provides an enhanced approach in contrast to previous literature that tests predefined scenario sets instead.

Moreover, the paper translates the changing pulse response under varying climatic conditions into a state-dependent TCRE. The state-dependent TCRE, once explicitly quantified, is used to develop a non-linear carbon budget equation. This equation is capable of replicating the temperature dynamics seen in a reduced-complexity climate model, also reffered to as a simple climate model (SCM). Therefore, it is shown that one can deduce the model's degree of carbon budget non-linearity, only by examining its pulse response. Moreover, an alternative way of deriving the non-linear carbon budget equation to that put forward by Nicholls et al. (2020). The novelty of the method given in this paper is that a user does not assume any functional form but derives the change of TCRE from the change of the pulse response under changing climatic conditions.

Lastly, the paper shows how different parametrizations of the model lead to different behaviour of the pulse response. Using the same logic as with inspecting the state-dependent TCRE, it is explained how the pulse response representation reveals whether a specific model's parametrization leads to concave, convex or linear carbon budget equation. This comes with a caveat since only a very limited parameter space has been inspected and the equation has been derived for only one parameter set. While the indications are clear, the validation accross a larger parameter space is left for future work.

Overall, this paper offers a fresh perspective on how to approach the carbon budget and its deviations through the pulse response lens. It presents the pulse response in the role of Green's function, providing a unifying view on both the scenario and state-dependence of the carbon budget approach.

The paper is arranged as follows. In Sect. 2, the models are introduced and the Green's function framework is connected with the carbon budget equation. In Sect. 3, the pulse response representation in the context of Green's function is inspected and its implications for scenario and state-dependent deviations are revealed. Additionally, Sect. 3 provides a method to derive a non-linear carbon budget equation using a changing pulse response as an approximation for state-dependent TCRE. In turn, Sect. 4 introduces the optimization program which generates the upper boundary scenario-dependent deviations and validates Green's approach; also, the non-linear budget equation is tested against the corresponding SCM. In Sect. 5, the findings are discussed in a broader context.

2 Models

The numerical optimization procedure introduced in Sect 4. used to validate the Green's approach and generate carbon budget deviations requires a substantial number of model runs, so a computationally efficient model is a necessary choice. Hence, we restrict this analysis to a class of simple climate models, also known as climate emulators. We distinguish between and apply two approaches, the SCM approach and its corresponding Green's function approach. While the former is sufficient for numerical assessment of the carbon budget deviations, the latter mathematically formalizes the carbon budget approach and

offers a fresh perspective on the deviation through the pulse response representation. All of the runs are executed in the GAMS programming language, and the code for all models and runs is available online (https://doi.org/10.5281/zenodo.8314808).

2.1 FaIR model

By FaIR, I am referring to the FaIRv2.0.0 model as provided by Leach et al. (2021). The Cross-Chapter Box 7.1 in IPCC AR6 WG1 argues in favor of FaIR's value as a climate emulator (Forster et al., 2021). For the purposes of this paper, two features of FaIR are crucial. The first is its ability to correctly capture the temperature response following a single carbon emission pulse, i.e., pulse response (Millar et al., 2017); the second is its ability to incorporate climate feedback on the carbon cycle, with one of the effects being the modification of the changing pulse response with changing climatic conditions.

In essence, the FaIR model is a SCM designed to emulate the gas dynamics of different radiative forcers and their effect on the global mean temperature. Because we are interested only in the deviations from the carbon budget, the non-CO_2 forcers are left out of the analysis, utilizing only the carbon cycle system and its radiative forcing dynamics. The model's description and equations can be found in Leach et al. (2021).

FaIRv2.0.0 consists of four carbon and three temperature components. Each carbon component has an associated decay timescale which dictates the dissipation of the carbon content into the shared permanent pool that represents the natural global carbon sink. Along with the global temperature increase, the sink's increased content creates a feedback mechanism, resulting in increased decay timescales and, therefore, increased atmospheric CO2 retention time. The atmospheric concentration gives rise to radiative forcing by combining a logarithmic and square root term, which translates into the temperature increase distributed between the components. Unless explicitly stated otherwise, FaIR is implemented with its default parametrization, with the default thermal and carbon cycle feedback parameters provided in (Leach et al., 2021), and with the default carbon cycle parameters presented in (Millar et al., 2017).

The effect of parameter uncertainty is addressed via a set of six FaIR calibrations. The parameters can be found in Tables 2 and 3 in (Leach et al., 2021), representing the thermal and carbon cycle feedback parameters tuned to CMIP6 models. Specifically, the sets used in this paper are tuned to the MIROC-ES2L (Hajima et al., 2020), BCC-CSM2-MR (Wu et al., 2019), MPI-ESM1-5 (Müller et al., 2018), CNRM-ESM2-1 (Séférian et al., 2019), and ACCESS-ESM1-5 (Ziehn et al., 2020) models.

2.2 The one-box model

To see how drastically different pulse response affects the deviation, another SCM is introduced into the analysis. Employed as a climate module in climate-economy integrated assessment models like FUND (Anthoff and Tol, 2014), PAGE (Hope, 2006), and MIND (Edenhofer et al., 2005), the one-box model consists of only one carbon and one temperature compartment, and it does not include any climate feedbacks. Since Joos et al. (2013) have shown that three to four timescales attributed to individual compartments are necessary to correctly approximate the redistribution of CO_2 in the atmosphere, the one-box model is not sufficient to imitate ESMs fully. Nevertheless, Khabbazan and Held (2019) have shown that different calibrations can be found with which it can emulate the temperature response of ESMs under RCP scenarios. The model's description and equations

can be found in Petschel-Held et al. (1999). In this paper, the thermal parameters were chosen to fit the TCR and ECS values provided by FaIR's default parametrization, with the conversion formulae given in Khabbazan and Held (2019).

Note that FaIR and one-box are not on equal footing, as the former is considered a state-of-the-art climate emulator, while the latter does not adhere to the carbon budget approach, as will be shown. Hence, the one-box model's pulse response should not be considered a correct representation of climate response, but rather a comparison tool. It is introduced in this article precisely because of its inexact pulse response behavior, in order to underscore how the pulse response is connected to carbon budget deviations. Also, it allows us to explore the effects of structural model uncertainty.

2.3 The Green's function framework

2.3.1 The Green's function formalism

Green's model is one equation motivated by Green's function formalism. Essentially, a Green's function $f_g(t-\tau)$ is a specific function unique to a set of linear differential equations $Lx(t) = y(t)$, where $y(t)$ is the input forcing and $x(t)$ is the state variable that changes according to the forcing and the linear operator L. The advantage of Green's function is that it acts as a 'propagator' from the input variable (external forcing) to the output variable (change in state variable), allowing us to replace differential equations with just one equation, which reads as $x(t) = \int_{t_0}^{t} y(\tau) f_g(t-\tau) d\tau$.

Using the same formalism, Green's equation is proposed in the context of global mean temperature dynamics with a climate model in lieu of a set of linear differential equations (see Raupach (2013)). Hence, we propose the following equation, imitating the Green's function formalism:

$$T(t) = \int_{t_0}^{t} E(\tau) f_g(t-\tau) d\tau. \tag{2}$$

The output variable is the global mean temperature change $T(t)$, and the input (forcing) variable is the emissions $E(t)$. Green's function $f_g(t-\tau)$ modifies the contribution to a current temperature $T(t)$ stemming from the past emissions $E(\tau)$. According to Eq. (2), the temperature in time t will depend on each emission contributing at time τ prior to t, with the effect modified by Green's function f_g dependent on how far the emission year τ is from t, hence $f_g(t-\tau)$. Essentially, it is an integration scheme that counts the temporarily modified temperature contributions to each emission pulse, going backwards from moment t, with a resulting temperature being a superposition of modified contributions. Similar approaches can be found in the literature in Shine et al. (2005) and Ricke and Caldeira (2014). The difference is that, in Eq. (2), the temperature is deduced directly from emissions, without the need for quantifying the radiative forcing and/or atmospheric CO_2 response.

2.3.2 The pulse response as Green's function

To make use of Eq. (2), one needs to choose an appropriate shape of Green's function f_g. Following the proposed definition, the chosen function is set to be a temperature evolution response following the 1 PgC emission pulse, or simply, the 'pulse response'. Therefore, in this paper, the terms 'Green's function', 'pulse response', and 'temperature evolution following the

emission pulse' are interchangeable. Pulse response experiments are one of the generic experiments applied when evaluating climate models. As done in previous literature (Joos et al. (2013), Millar et al. (2017)), the pulse response is generated by adding a unit emission pulse on prescribed emissions that keep a constant background atmospheric concentration background, as follows.

The model is forced by the idealized RCP6.0 CO_2-only emission scenario provided by the RCMIP protocol (Nicholls, 2021), starting from the year 1850. In the year of pulse response generation t_p, the emission pathway necessary to keep the level of atmospheric concentration $C_a(t_p)$ constant is generated. Using the derived emissions, two experiments are run: One with the generated emissions only and one with 1 PgC extra added in t_p. Thus, the pulse response (Green's function) is determined by subtracting the temperature evolution of the two runs.

The pulse response functions generated for different years (and hence, different climatic conditions) can be found in Figs. 1a, 1b, and 3, for the FaIR model standard parametrization, one-box model, and different FaIR parametrizations, respectively. In this paper, the set of different pulse responses generated under different climatic conditions is named a *pulse response representation*. Having a set of pulse responses (a representation) gives us information on both scenario- and state-dependency of a particular model, as will be discussed in the next section.

The Green's functions f_g utilized in Green's model (Eq. (2)), and used in the optimization programs in Sect. 4, are generated at the year $t_p = 2020$ and depicted in blue in Figs. 1a and 1b, labeled 'pulse2020'.

3 Pulse response as carbon budget deviation indiciator

In this section, the theory behind the pulse representation in form of Green's function and its ability to explicate carbon budget deviations is explored. The scenario-dependency is connected with the shape of the pulse response, whilst the state-dependency with changing of the pulse response under changing climatic conditions. The conclusions are validated numerically in Sect. 4. Firstly, the connection between Green's function (Eq. (2)) and carbon budget equation as suggested by Eq. (1) is examined, showing that the latter is merely a special case of the former.

3.1 The carbon budget equation in the context of Green's formalism

Essentially, the linear carbon equation (Eq. (1)) suggests an immediate temperature response to (cumulative) emissions, with the response that does not change in time or with climatic conditions. This implies that the pulse response introduced in the previous subsection should also be a constant function. In Fig. 1a, it is plotted as a dashed black line. Formally, a linear budget pulse response can be interpreted as a Heaviside function $\Theta(t)$ multiplied by a constant equal to Λ representing TCRE:

$$f_g^0(t-\tau) = \Lambda\Theta(t-\tau) = \begin{cases} 0 & t < \tau \\ \Lambda & t \geq \tau \end{cases}, \tag{3}$$

where τ is the timing of the emission pulse and is equal to the 0th year in Fig. 1.

| (a) Default parametrization FaIR | (b) One-box model |
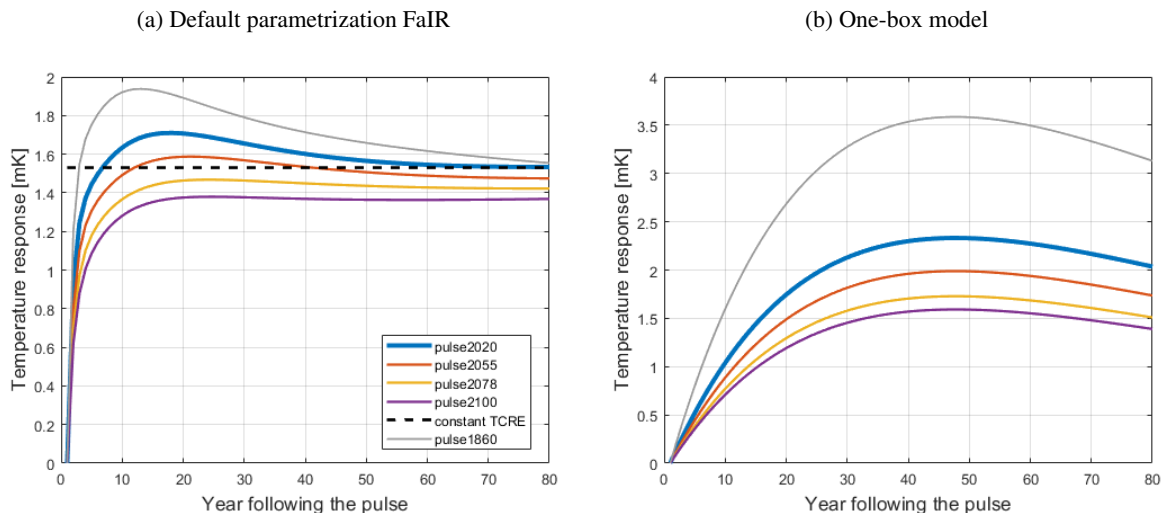
Figure 1. Temperature evolutions in response to 1 PgC emission pulse for different climatic conditions, i.e., pulse responses (colored lines), and the temperature response implied by Eq. (1) (black dashed line). The numbers correspond to the year of an idealized RCP6.0 scenario in which the pulses were generated. Years 2020, 2055, 2078 and 2100 correspond to the FaIR generated background temperatures of 1, 1.5, 2 and 2.5 K, respectively, and 1860 to preindustrial climatic conditions. Constant TCRE is equal to 1.53 K EgC^{-1} and corresponds to the central TCRE estimates in Leach et al (2021) and AR6, respectively.

Proving that the Green's formalism can be considered an analogue to the carbon budget approach is simple. Inserting the idealized budget Green's function into Eq. (2), one arrives precisely at the linear budget equation (Eq. (1)):

$$T(t) = \int_{t_0}^{t} E(\tau) f_g^0(t-\tau)\mathrm{d}\tau = \int_{t_0}^{t} E(\tau)\Lambda\Theta(t-\tau)\mathrm{d}\tau = \Lambda \int_{t_0}^{t} E(t')\mathrm{d}t' = \Lambda F(t).$$

220 Therefore, if the temperature response always had the same (constant) shape as the dashed line in Fig. 1, regardless of the underlying climatic conditions, the carbon budget would not show deviations – each unit of carbon emission would immediately add to the warming equally and regardless of when it was emitted. However, as shown in Fig. 1, the FaIR-generated pulse responses are not a constant function, a fact that has implications for the carbon budget deviations.

3.2 Pulse response shape as a scenario dependency indicator

225 For now, the focus is on the pulse response functions that is used in Green's model (pulse 2020, Fig. 1a). In contrast to a constant step function, the initial response at the year of the emission pulse is zero. Then it steeply increases until reaching a maximum value of approximately 1.7 K, roughly 17 years following the pulse. Furthermore, following the peak, there is a slow relaxation of the response, which slowly reaches a constant response later in time.

To get a better feel for the deviations and how they are connected to the pulse, one can consider an extreme example. Say that all of the emissions are injected in one year. Total cumulative emissions will then amount to the value of the emissions injection only. Due to the pulse response, the temperature response will depend on what point in time the observer is at. Tracing the pulse response evolution, we can see a minimum magnitude of temperature in the first year of the pulse and the maximum temperature at the peak of the response, $\sim$17 years after the pulse. Effectively, these are two very different temperatures for the same cumulative emissions. The difference between the two temperatures is the maximum possible scenario-dependent carbon budget deviation. If the cumulative emissions then amount to 100 PgC, the pulse response scales accordingly, and the theoretical deviation between the minimum and maximum response is ~0.17 K.

Finally, because of the gradual relaxation of the response, if the year in question is far enough from when we maximized the deviation, the deviation itself diminishes. In the extreme case presented in the previous paragraph, this can be intuitively seen as follows. Although there could have been a considerable difference in temperature stemming from the same cumulative emissions between the 0th (the injection year) and 17th year (the peak year) following the pulse, going forward in time, the temperature response difference between the 80th and 63rd year following the pulse (again, a 17-year difference) is virtually non-existent. Hence, the carbon budget deviation 'fixes' itself as the system enters dynamic relaxation, i.e., the pulse response reaches a nearly constant value. Once it reaches the relaxation phase, the pulse response becomes very similar to the step-function response of the linear budget.

The Green's function derived from the one-box model is shown in Fig. 1b (blue). Unlike its FaIR counterpart, the one-box model's pulse response peaks much later (roughly 45 years after the pulse). Additionally, and more importantly, it never reaches the relaxation phase in the form of a constant response in later years; it starts permanently decreasing after the peak instead. In the context of the discussion above, this means that, aside from its magnitude, even the sign of the one-box model's scenario-dependent deviations can change depending on the relative time we observe it. Repeating the thought experiment above, where we emit everything in one year, the observer will see a positive deviation comparing the initial (injection) year and the peak year ($\sim$45 years difference). If we go forward in time, specifically 45 years farther, the observer who was in the initial year now sees their temperature response at the peak, while the observer who was in the peak temperature year now sees a much lower temperature. Subtracting the two now yields a negative value, even though the deviation was previously positive.

In summary, the pulse response shape dictates both the deviation and its evolution, making it critical for the climate model's adherence to the carbon budget approach and its emission scenario independence. The FaIR model shows small, scenario-dependent deviations precisely because its pulse reaches an almost constant regime relatively quickly following a peak. Moreover, if a model cannot emulate reaching the temperature relaxation, it will also show much higher and more importantly, time-dependent emission scenario-dependent deviations.

3.3 Pulse response alteration as a state-dependency indicator

Until now, only a single pulse response (pulse2020) has been employed as Green's function and examined. However, the experiment shows that this pulse response changes with changing climatic conditions: Following the same procedure described in 2.3.2, pulse responses are generated later in the RCP emission run, for different t_p's accordingly. The generated pulses are

depicted in different colors in Fig. 1 for both the FaIR and one-box models. The further analysis considers only the FaIR results, as the one-box model fails at criteria of pulse response relaxation, explored in the previous subsection.

When comparing the pulses (Fig. 1a), a general trend can be recognized. As the system is subjected to higher climatic stress in the form of higher cumulative emissions and higher temperatures, both the shape and the magnitude of the pulse response change. While all the pulse response variations show the aforementioned steep increase in the first few years following the pulse, the magnitude of the peak and the corresponding relaxation temperature level decrease with changing climatic conditions, with a visible 'flattening' of the curve.

3.3.1 State-dependent pulse response as a variable TCRE

As discussed in the introduction, the previous literature suggests that TCRE is not a constant value but slowly decreases with cumulative emissions. This can be interpreted as the carbon budget's state-dependency, which manifests in the non-linear carbon budget equation (Nicholls et al., 2020). This non-linearity can be identified by examining the change in pulse response shape with changing background climate conditions.

At the beginning of Sect. 3, it was shown how the step-function pulse response in Green's model translates into TCRE included in Eq. (1). If the TCRE changes with background conditions, the carbon budget step-function pulse (black dashed line, Fig. 1) should also change in magnitude following the climatic stress. Indeed, Fig. 1 shows that the FaIR-generated pulse response decreases in magnitude with background conditions. If then the changing pulse is approximated with a changing step function, the decrease of the pulse response can be directly linked to the decrease of TCRE. A method for using a pulse response representation to explicitly quantify TCRE dependency on climatic conditions is developed, as follows.

To generalize the analysis, the additional pulses are generated under RCP4.5 and RCP8.5 emission scenarios, along with the already generated pulse responses under different climatic conditions under RCP6 (Fig. 1). The first pulse of each run is generated at the benchmark year 2020 and the rest at the same temperature levels (1.5, 2 & 2.5 K), where possible.

Next, recalling the linear budget discussion, the generated pulses are to be approximated with the step function. Ignoring the temperature evolution dynamics in the early years of the pulse response, the pulse is transformed into a constant Λ_v by averaging it between years 70 and 80[2]. As shown in Fig. 1, the pulse dynamics relax by that time, reaching relative constancy. With that approximation, however, the ability to express the time delay and scenario dependency is lost, as the shape of the pulse response function dictates the scenario dependency (Sect. 3.2). As they will be shown to be small, this aspect can be safely ignored.

After approximating the pulses, the corresponding cumulative emissions and temperature values (i.e., the background climatic conditions under which the original pulse was generated) are assigned to each value of generated Λ_v. By doing so, the $\Lambda_v(T,F)$ dependency is mapped, which, when reasoned in line with Eq. (1)[3], can be considered a TCRE dependent on cumulative emissions and temperature increase, or simply, state-dependent TCRE.

---

[2]In this way, the approximation for each pulse resembles the black dashed line in relationship to the blue line in Fig. 1.

[3]Note that Λ and Λ_v have the same function in the carbon budget equation. The difference is that Λ is a constant, while Λ_v is a function of temperature and cumulative emissions.
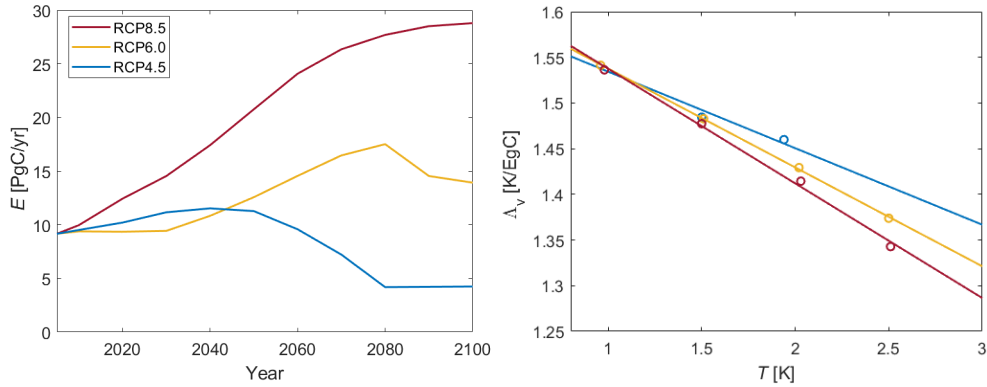
Figure 2. Right graph: TCRE approximations $\Lambda_v(T)$ generated from pulse response functions under different climatic conditions and emission scenarios. Scatter plots are actual values of Λ, while the line is the result of linear regression. The different colors represent the Λ_v's generated from different RCPs, which are plotted in the left graph.

In this way, the carbon budget's state dependency is made explicit: Examining each RCP case separately shows that Λ_v decreases linearly in T under the standard FaIR parametrization (Fig. 2b). Moreover, looking at the right figure, one can see that by adding 1 EgC into the system, $\Lambda_v(F)$ drops by roughly 10%, which is in keeping with the findings of Leach et al. (2021).

3.3.2 From pulse response to carbon budget equation

The RCP6-generated Λ_v (Fig. 2b, yellow dots) is chosen to derive the carbon budget's state dependency from the pulse response representation. The choice of RCP scenario does not constrain the conclusions of this exercise. Fig. 2b suggests a linear relationship $\Lambda_v(T) = -\mathrm{a} \cdot T + \mathrm{b}$, with $\mathrm{a} = 0.1083$ EgC^{-1} and $\mathrm{b} = 1.646$ K EgC^{-1} derived via linear regression. Therefore, TCRE (here Λ_v) is reinterpreted through the lens of T dependency, as temperature is the main thermodynamic variable driving the climate system change. This way, assuming any functional form for the state depenency is avoided; rather, it is deducted from mapping $\Lambda_v(T)$ (Fig. 7, right graph). The assumed linear relationship between TCRE and T suggests that TCRE can go to very low, and even negative values due to the negative linear coefficient. However, the linear form is derived and holds true for the values below 2400 PgC (approximately the cumulative emissions in RCP8.5 scenario at the year 2100). Hence, its domain of applicability is constrained within the theoretical TCRE bounds of 2000 PgC. Additionally, one can see that the assumed linear relationship suggests TCRE would reach zero at roughly $T = 15$ K, well above any projected future temperature increase.

Since Λ_v is, by definition, a temperature response to an emission pulse, the temperature change following the approximated pulse is interpreted as $\Delta T = \Lambda(T) \cdot E_{pulse}$. In words, the temperature change is equal to one unit of pulse emission scaled by temperature response to a pulse Λ_v. Given the fact that the emission pulse brings about a change in cumulative emissions, the

aforementioned relation is rewritten in differential form as:

$$dT = (-a \cdot T + b)dF. \tag{4}$$

315   By integrating Eq. (4), one arrives at:

$$T(F) = \frac{b}{a} + (T_0 - \frac{b}{a})e^{-a(F-F_0)}, \tag{5}$$

with T_0 and F_0 being the initial values at the time of the first pulse (pulse2020). Essentially, Eq. (5) represents a non-linear carbon budget equation under a default FaIR parametrization. The validity of the equation is tested in Sect. 4.

    When plotted, one can see that $T(F)$ is a closely linear, slightly concave function within the F domain of interest[4]. Concavity
320   comes from the (linearly) decreasing $\Lambda_v(T)$ (Fig. 2b). If, conversely, $\Lambda_v(T)$ increases with increasing T, the same derivation method as presented above would lead to a convex carbon budget equation. As will be shown in the next subsection, this is possible as pulse response, and subsequently $\Lambda_v(T)$, evolves differently under different FaIR parametrizations.

3.4   Uncertainty in pulse response

By considering the pulse response representation and its implications on the carbon budget framework under one FaIR
325   parametrization, the effects of different model calibrations on pulse response and, thereby the carbon budget are evaluated in the final part of this section.

    Fig. 3 shows pulse responses generated as described in 2.3.2 under six different sets of FaIR parameters, each tuned to a different CMIP6 model, with Fig. 9e being the default parametrization used in the rest of the analyses. We can see that every calibration yields a distinct pattern of behavior. Using the framework introduced in the previous parts of this section, one can
330   deduct how each calibration affects FaIR's adherence to the carbon budget approach.

    To examine scenario dependency, one must examine pulse response shape (Sect. 3.2). Looking at Fig. 3, we can see that all of the parametrizations show a relatively small scenario dependency, as all of them show pulse responses that peak in 10-20 years, followed by some degree of relaxation in the time domain of interest. In other words, one can imagine approximating them with a step function. Two parametrizations that stand out are MIROC-ES2L and ACCESS-ESM1-5. The former reaches a
335   peak and then continually decreases just like the one-box model, although at a much slower rate (Fig. 1b). Hence, the scenario-dependent deviations will not fully diminish and are likely to change sign. The same holds true for the latter, although in the other direction as the pulse response of ACCESS-ESM1-5, as the temperature gradually increases following the pulse.

    In the context of state-dependent deviations, Fig. 3 reveals an interesting effect of different FaIR parametrizations on the non-linearity type of carbon budget equation. In Sect. 3.4, it was shown that the changing TCRE under different climatic conditions
340   can be reinterpreted as the changing pulse response through $\Lambda_v(T)$. Additionally, it was shown that a decreasing $\Lambda_v(T)$ (Fig 2b) leads to a concave non-linear carbon budget equation (Eqs. (5) and (6)). The opposite also holds true: If $\Lambda_v(T)$, and hence the pulse response increases in magnitude with higher temperatures, it results in a convex non-linear carbon budget equation.

---

[4]Note that here F represents the total cumulative emissions from the preindustrial era. One could rewrite the equation with $\Delta F = F - F_0$ to derive the temperature increase relative to the initial year $t_0 = 2020$.
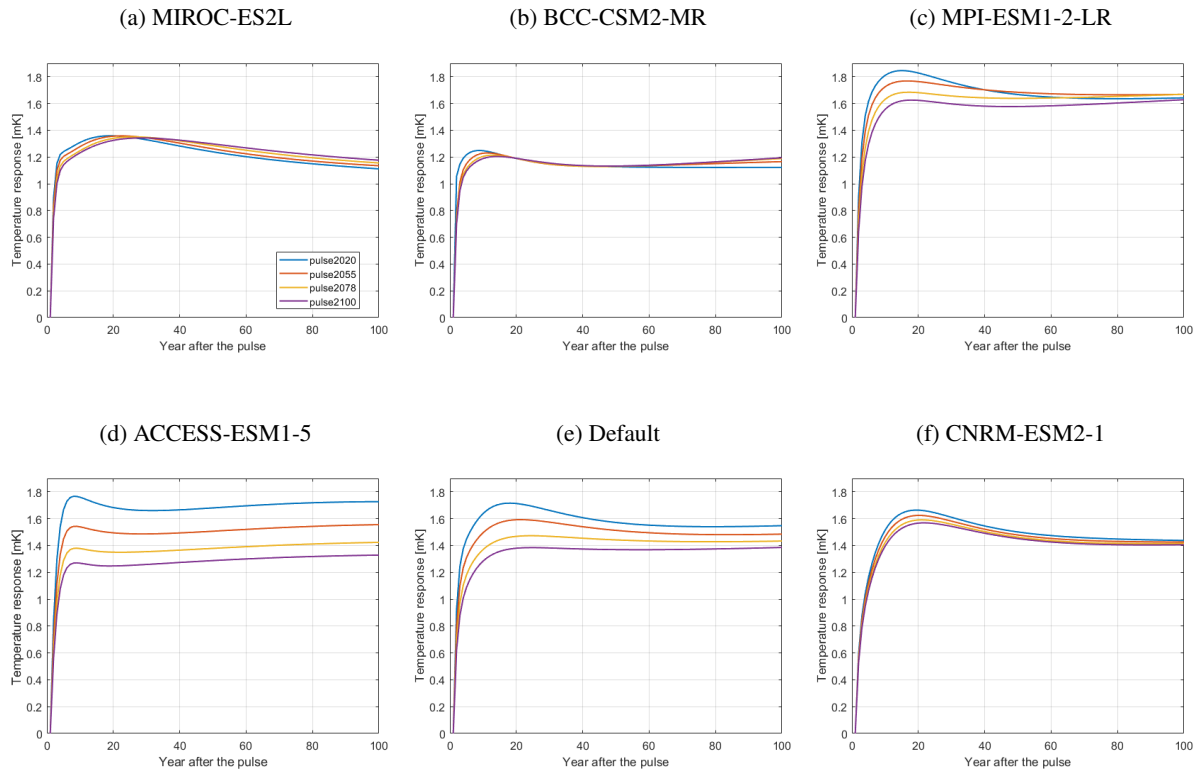
Figure 3. Pulse responses under different FaIR calibrations. Different parameter sets are each tuned to a specific ESM, with parameter values given in Tables 2 and 3 in Leach et al. (2021). Note that graph (e) matches the left graph in Fig. 1, included here for comparison.

Ultimately, if the pulse response magnitude does not change with changing background conditions, the carbon budget equation is indeed linear[5]. With that in mind, one can easily deduct that not all the combinations of FaIR parameters lead to the concave

345   carbon budget equation, as derived in Eq. (6). For example, MIROC-ES2L tuned to FaIR indicates a slightly convex budget equation, while BCC-CSM2-MR and CNRM-ESM2-1 are closest to the linear carbon budget, while ACCESS-ESM1-5 shows larger concavity then the default FaIR setup inspected in the previous subsection.

Due to the constrained set of fully accessible parameter sets given in Leach et al. (2021), only six calibrations are presented here. A larger set would provide some insights into which parameters in FaIR drive which types of behavior. Additionally,

350   it would be interesting to see to which extent FaIR tuned to a CMIP6 model reproduces the pulse response representation behavior of its corresponding ESM under the same setup. To do so, one needs to run the pulse response experiments (Fig. 3) with ESMs. If it were found to do so, one could potentially extend the pulse response framework with FaIR tuned to ESMs to analyze carbon budget deviations as produced by the corresponding ESM.

---

[5]Note that a pulse relaxation is still a necessary requirement.
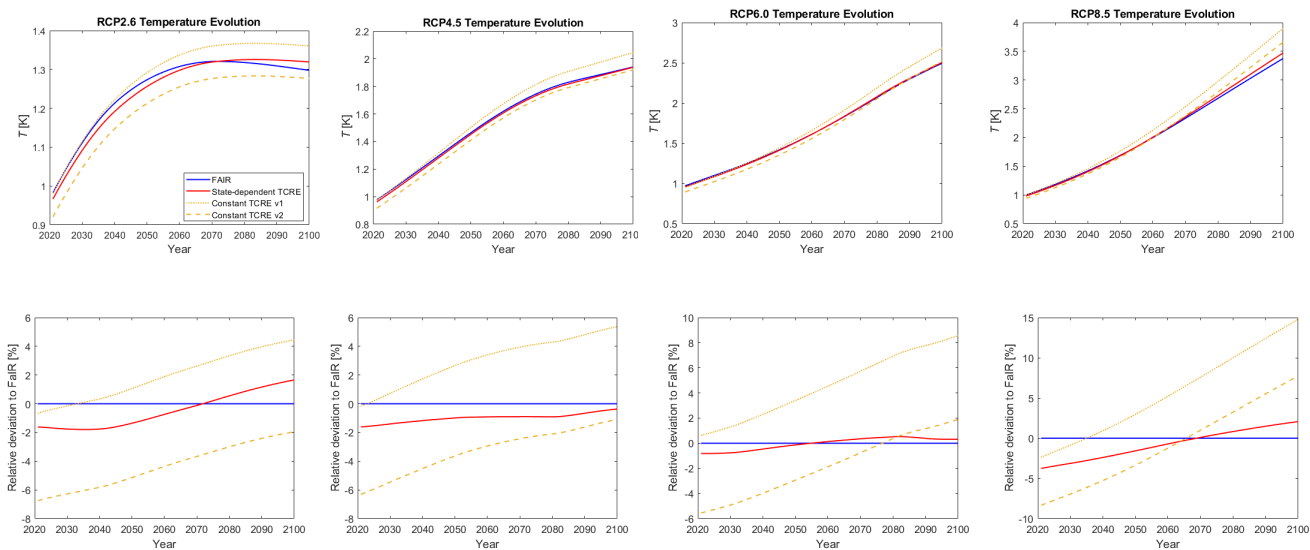
Figure 4. Top row: Temperature evolution under three RCP emission scenarios, calculated by FaIR model (blue), the derived non-linear carbon budget equation (Eq. (6)) (red), and the linear carbon budget equation (Eq. (1) with two different TCRE values) (yellow). Bottom row: Corresponding relative deviations of generated temperatures from FaIR-generated temperature, in percentages.

4   Numerical evaluation

355 In the previous section a theoretical background for inspecting carbon budget deviation through the lens of pulse response was established. The shape of the pulse response function is assumed to give information about the model's scenario-dependent deviations, and the method for deriving the non-linear carbon budget equation from the changing pulse response with changing climatic conditions is provided. In the first, brief part of this section, the state-dependent (non-linear) carbon budget equation is tested against its linear counterpart and FaIR. For the rest of this section the results of using an optimization scheme are

360 presented. Using the optimization scheme in this context has a twofold role. Firstly, the pulse response's ability to capture scenario-dependent effects in a role of Green's function is confirmed with comparison to the corresponding SCM, validating the hypotheses given in the previous section. Secondly, the optimization scheme tests the full portfolio of possible emissions, providing the highest possible scenario-dependent deviation under given constraints.

The appendix introduces a modification to Green's function approach that is necessary to compare diagnosed temperatures

365 in the upper panels of Fig. 5 (but not scenario-dependent deviations, lower panels) between Green's approach and the FaIR model. The modification is a temperature leftover from emissions prior to an optimization year and is, in fact, ZEC (Appendix A).

4.1 State-dependent carbon budget equation

To check if Eq. (5) yields correct temperature dynamics, it is tested against the FaIR model under the aforementioned RCP scenarios. The resulting temperature pathways are plotted in the top row of Fig. 4 (red) alongside the FaIR output (blue) and the linear carbon budget Eq. (1) with two values of constant TCRE (yellow), while the bottom row shows the corresponding relative deviations from the FaIR-generated temperature pathway. The two TCRE values are $\mathrm{TCRE}_{v1}=1.6\cdot10^{-6}$ K PgC^{-1}, and $\mathrm{TCRE}_{v1}=1.53\cdot10^{-6}$ K PgC^{-1}.

Choosing a larger constant TCRE (v1) results in a more accurate temperature diagnosis in the first half of the century under lower cumulative emissions, with deviations increasing in step with rising emissions. The opposite is true for a smaller TCRE. In this sense, Eq. (1) with a constant TCRE is a linearized version of FaIR in a similar way as the Green's function model but without the ability to generate scenario-dependent effects. Additionally, we can see that the state-dependent deviations are not transient like their scenario-dependent counterparts, but ever-increasing with the changing cumulative emissions. The highest detected absolute deviation is around ~ 0.5 K for the end-of-the-century temperatures in the RCP8.5 run, which amounts to $\sim 15\%$ relative deviation from the FaIR-generated temperature.

Unlike constant TCRE, Eq. (5) replicates the FaIR generated temperatures in RCP2.6, RCP4.5, and RCP6 runs relatively well, with the relative deviation from FaIR being less than $\sim 2\%$ throughout the century. The largest absolute drift from the FaIR-generated temperature is around 0.1 K at the end of the century under the RCP8.5 scenario. However, this degree of drift is less than 3% in relative terms. Since RCP8.5 is arguably somewhere in the upper bound for possible emission pathways (and RCP2.6 arguably a very optimistic lower bound scenario), one can conclude that Eq. (5) is a good emulator of FaIR under the single, default parametrization. The incorporation of different climate parameters in Eq. (5) lies beyond the scope of this paper.

4.2 Scenario-dependent deviations

4.2.1 Optimization scheme

To test upper-bound scenario-dependent carbon budget deviations, the optimization program is formulated as follows:

$$(\text{Max}, \text{Min})[T(t^*)] \quad \text{s.t.} \int_{t_0}^{t^*} E(t)\mathrm{d}t = F_{\text{tot}}, \; \left|\frac{\mathrm{d}E(t)}{\mathrm{d}t}\right| \le k, \; E(t) \ge 0, \; E(t_0) = E_0. \tag{6}$$
$$\{E(t)\}$$

The program maximizes (or minimizes) the temperature variable in a given optimization year t^*. The minimum $T_{\min}(t^*)$ and maximum $T_{\max}(t^*)$ temperatures generated provide the upper and lower bounds for possible temperatures under given constraints. The maximum possible scenario-dependent carbon budget deviation T_{d} is then calculated by subtracting the two boundary temperatures, $T_{\mathrm{d}}(t^*) = T_{\max}(t^*) - T_{\min}(t^*)$.

In the optimization program (Eq. (6)), the emission pathway assumes the role of the free control variable, except in the fixed initial condition $E(t_0) = E_0$. Hence, the novelty of testing scenario independence with the optimization program is that the emission pathway is generated, instead of being assumed as an input by the user. This way, the analysis does not rely on a limited number of emission scenarios but systematically runs through the whole portfolio of possible scenarios under
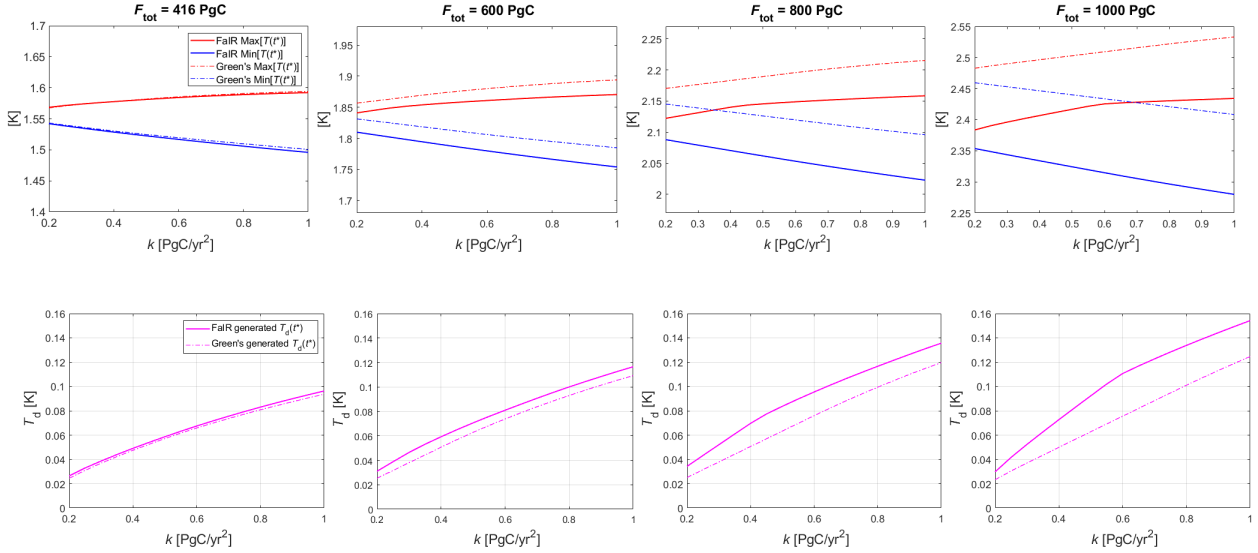
Figure 5. Top row: $T_{\max}$ (red) and $T_{\min}$ (blue) generated by the optimization program for the transient budget case, dependent on k, set up for different total cumulative emissions levels F_{tot} and $t^* = 2090$, with F_{tot} counted from the initial optimization year $t_0 = 2020$. The graphs are ordered by the magnitude of the associated F_{tot}. Y-axis domains all share the same relative interval of 0.3 K, but different absolute values. Lower panels: corresponding scenario-dependent deviations T_d plotted against the respective k values. In all graphs, the solid lines represent the FaIR output; the dashed lines represent Green's output.

given constraints. Three boundary conditions are implemented, whose values are subjectively chosen by the author, so that
400   they provide a set of possible (not necessarily plausible) emission pathways. Restriction on total cumulative emissions F_{tot}
ensures the same amount of cumulative emissions at the end of the each run, so that deviations stem only from scenario choice.
The slope restriction k provides a bound on allowed emission change per year. The choice of boundary conditions and run
configuration is further described in the supplementary material (S1).

    Additionally, two different cases of scenario-dependent deviations are diagnosed and described in the supplement. The "net-
405   zero" case assumes that the emissions reach zero and that there are no emissions following the optimization year, while the
"transient budget" case allows for emissions to evolve freely afterwards and allows for emissions to take any value in the
optimization year.

4.2.2   Transient budget deviation

In Fig. 5, the results of the optimizer in $t^* = 2090$ for four different F_{tot} choices in a transient budget setup are presented,
410   explicitly showing the generated $T_{\max}(t^*)$ and $T_{\min}(t^*)$ dependent on k in the top row and and their corresponding $T_d(t^*)$
values in the bottom row. Note that F_{tot} are counted from the year $t_0 = 2020$, and not from preindustrial times like the variable
F. For example, F_{tot} of 416 PgC, in addition to the pre-2020 emitted CO_2, amounts to 1000 PgC, which approximately
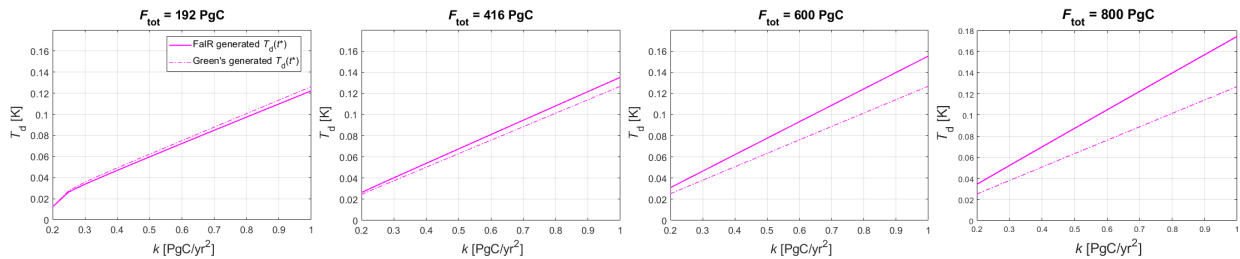
Figure 6. Scenario-dependent deviations, dependent on k, generated by the optimization program for the transient budget case with the allowed negative emissions, dependent on k, set up for different total cumulative emissions levels F_{tot} and $t^* = 2090$, with F_{tot} counted from the initial optimization year $t_0 = 2020$.

corresponds to the carbon budget allowed for adhering to 2 K increase with 67% probability, as suggested by the IPCC (Masson-Delmotte et al. (2021), Table SPM.2)[6].

415   Comparing the dashed and solid lines reveals that Green's approach using the pulse response as a Green's function diagnoses both T_{max} and T_{min}[7], as well as scenario-dependent deviations, exhibiting deviations of the same order of magnitude as FaIR, with the Green's function approach being especially close to FaIR for lower cumulative emissions.

     When comparing the effect of increasing cumulative emissions in Fig. 5, some notable effects can be identified.

     First, $T_{\text{d}}(k)$ increases with higher cumulative emissions, in combination with the increase due to increasing allowed emission

420 slope k. A comparison of the top to bottom graphs shows that the deviation increases by roughly 60%, in connection with the F_{tot} increase from 416 PgC to 1000 PgC. In the most extreme case with associated $F_{\text{tot}} = 1000$ PgC, a deviation of ~ 0.15 K, roughly 6.3% of overall temperature increase, is produced.

     Next, as seen in the top row, the gap between FaIR's and its Green's counterpart's generated T_{max} and T_{min} steadily increases with higher cumulative emissions F_{tot}[8].

425   Furthermore, as shown in the bottom row, the difference in $T_{\text{d}}(k)$ between the two models also increases with higher F_{tot}, albeit to a lesser extent. This effect can be attributed to the widening gap between the maximum and minimum temperature of the FaIR approach, which increases its $T_{\text{d}}(k)$ to a larger extent than does Green's model (due to the constancy of Green's function). Both effects can be understood through the change of pulse response with changing climatic conditions. Namely, Green's approach uses one single pulse response as a Green's function throughout the run, albeit the pulse response changes

430 under changing climatic conditions, i.e., higher cumulative emissions. The change in magnitude of the pulse response affects the drift between the FaIR and Green's generated T_{max} and T_{min}, while the flattening of the response peak causes the drift between the diagnosed deviations T_d's.

---

[6]The generated temperatures are lower due to exclusion of non-CO_2 forcers and the choice of parametrization.

[7]Refer to the appendix for modification of Green's function to make this comparison possible.

[8]Note that the y-axis domains all share the same relative interval of 0.3 K, but different absolute values. In this way, the focus is shifted to the changing difference between the Green's model-generated and FaIR-generated temperature with increasing F_{tot}.

4.2.3 Effect of negative emissions

The effect of allowing negative emissions on the transient budget's scenario-dependent deviation is shown in Fig 6. The figure
shows four different combinations of total allowed cumulative emissions F_{tot}, this time including a choice of $F_{\text{tot}} = 196$ PgC,
which, when added to the cumulative pre-optimization emissions, reflects the carbon budget allowed for adhering to 1.5 K
with 67% probability, as suggested by the IPCC (Masson-Delmotte et al. (2021), Table SPM.2). Including negative emissions
increases the generated T_d by roughly 0.04 K compared to the zero negative emissions scenario, in the highest k case for all
F_{tot} combinations.

4.2.4 Scenario-dependent deviation time evolution

Because the optimization program, when set up as net-zero case, does not allow for emissions following the optimization year,
it makes it possible to inspect the time evolution of the generated scenario-dependent deviation $T_d(t^*)$, as there are no further
emissions to further modify the temperature.

Figs. 7a and 7b show net-zero generated $T_d(t^*)$ with an additional, temporal dimension, instead of only k dependence in
one year (Fig. 5 (lower panels) and Fig. 6). In this case, the optimization year is chosen to be $t^* = 2070$. The different shades
of red depict the k range and their respective scenario-dependent deviations. The chosen F_{tot} for the run shown in Fig. 7 is 416
GtC.

The net-zero budget case shows a significantly smaller initial $T_d(k)$ than its transient budget counterpart. The difference is
due to lower minimum generated temperatures in the transient budget case, as a result of a non-constrained $E(t^*)$ and hence
allowing emissions to 'stack up' at the optimization year, while they are required to reach zero in the net zero counterpart.
The pulse response discussion (Sect. 3) shows that if one wants to maximize the temperature response in a given year, they
should stack the emissions ~ 17 years before that year; conversely, to minimize the temperature response, they should stack the
emissions as close as possible (within given constraints).

Further inspecting Fig. 7a one can notice that, in FaIR, already small scenario-dependent deviations ultimately disappear if
no additional carbon dioxide is added to the system; hence, the maximum deviations generated by the optimization program
are only temporary. In contrast to FaIR, the one-box model's deviations (Fig. 7b) do not 'die out' over time but decrease only
to change sign, as predicted in Sect 3.2.

The deviations' evolutions for $k = 1$ can be backtracked by examining the max. (red) and min. (blue) generated temperature
evolutions shown in Figs. 7c and 7d, as the subtraction of the two yields the $T_d(k)$. The FaIR-generated min. and max. temper-
ature pathways are separated at t^* but eventually coincide, translating to a diminishing carbon budget deviation. Even though
two temperatures are generated, they eventually reach the same level, just as the pulse relaxation discussed in the previous
section suggests they should. Additionally, their cumulative emissions are equal, meaning that their pulse response is the same,
so they reach the same level of constancy following the peak temperature response. The opposite is true for the one-box model
counterpart. Because the one-box model's pulse response never reaches relaxation phase, i.e., keeps on decreasing following
the peak, it makes a difference when we emit.
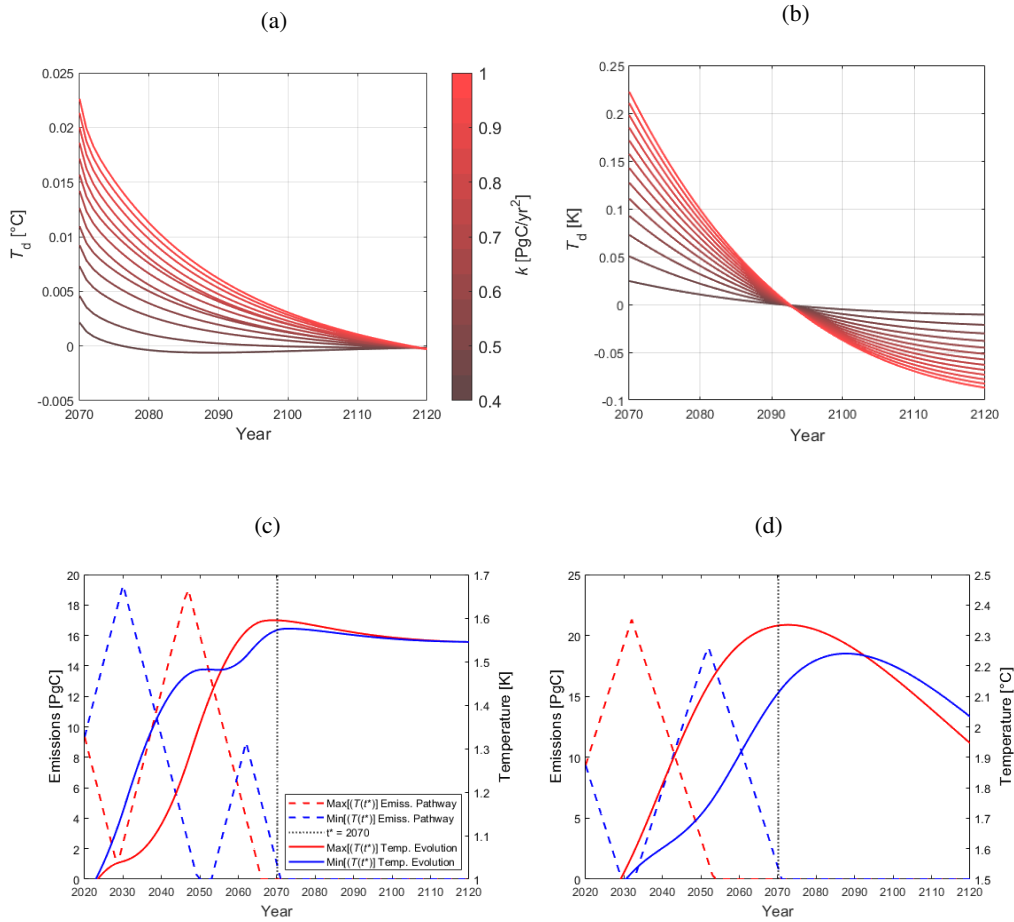
Figure 7. Graphs (a) and (b) show the temporal evolution of the net zero-case $T_d(k)$ following the optimization year $t^* = 2070$, generated by FaIR and the one-box model respectively. The colors represent deviations corresponding to the different k allowed, with the darkest red being the lowest allowed (0.4 PgC yr^{-2}) and the brightest red being the highest (1 PgC yr^{-2}). The generated emission pathways and absolute temperature evolutions corresponding to the optimization runs (both min. & max.) under the same setup for one value $k = 1$ PgC yr^{-2} are shown in graphs (c) and (d), generated by FaIR and one-box respectively.

5   Discussion

To reiterate, this study focuses on evaluating deviations within the carbon budget approach, encompassing both its scenario- and state-dependent aspects. A novel method of analyzing these deviations is proposed in the form of a pulse response representation that explicates and distinguishes both forms of deviations by inspecting the evolution of temperature response to an emission pulse under different climatic conditions. The validity of examining the deviations through the lens of the pulse response has been tested by reinterpreting the pulse response as a Green's function of a set of differential equations that constitute a climate model (Raupach, 2013). Consequently, the introduced optimization program serves a dual role. It supplements the concurrent carbon budget literature by testing a full portfolio of possible, but not necessarily plausible, scenarios for scenario-dependent deviations under given constraints. Additionally, it confirms the ability of Green's function to capture scenario-dependent effects.

The analysis utilizes FaIR, the one-box model, and the associated Green's function models. The non-linearities appear in FaIR in both the carbon cycle feedback and in the temperature response saturation. As pointed out in the introduction, the interplay between the changing carbon cycle and temperature response produces the near-linearity of the carbon budget equation, with the former being convex and the latter a concave driver of the budget equation.

The second model used in the analysis is the one-box model, introduced as an example of a model with a dramatically different pulse response than FaIR, which facilitates comparison in the context of the pulse response behaviour effect on the carbon budget approach deviations. In contrast to FaIR, the one-box model does not include climate feedbacks on the carbon cycle, so non-linearities arise only through the saturation in temperature response, which means that non-linearities are solely concave.

Moreover, the inclusion (or lack) of climate feedbacks has an effect on how the pulse response changes with changing climatic conditions. In the one-box model, the carbon cycle response stays the same regardless of background conditions, so the pulse response is modified only by logarithmic temperature response saturation. This manifests in the pulse changing magnitude but not shape. Conversely, including climate feedbacks changes the shape of the response function and modifies its magnitude. For a more detailed discussion on how the climate feedback changes the carbon cycle in FaIR in the context of decreased atmospheric CO_2 decay, see Millar et al. (2017). The effect of convex and concave drivers in context of pulse response representation and the non-linearities of the carbon budget equation (Eq. (1)) has been examined in Sect 3.4.

To test whether pulse response behavior offers a trustworthy framework for explaining carbon budget deviations, it is employed as a Green's function in Eq. (2). However, by proposing Eq. (2) and using a FaIR-generated (or one-box-generated) Green's function, we assume that the climate model is a set of linear differential equations. Hence, although Green's model has been proven to capture scenario-dependent effects, the effects of climate change on the carbon budget approach cannot be explicitly captured with Eq. (2). This effect is visible when comparing the FaIR's and Green's model optimization runs, as the two sets of generated temperatures have an ever-increasing gap with higher cumulative emissions (Fig. 5, top row). One could modify Eq. (2) so as to include a changing pulse response instead of a fixed f_g, but this remains theoretical; the implementation is unclear.

500   Regardless of Green's model's inability to correctly forecast (or hindcast, for the same reasons) temperature evolution, Sect. 4 shows that it is indeed capable of mimicking the scenario-dependent deviations of both FaIR and the one-box model. Even though there is an ever-increasing gap between temperatures generated by the SCM model and Green's model, the scenario-dependent deviations are well represented by Green's function even for higher F_{tot}. Hence, one concludes that state and scenario dependencies can arise independently.

505   The distinction is crucial because non-linearities in the carbon budget and scenario-dependent deviations are distinct concepts, yet both contribute to carbon budget deviations individually. The key proposition is that state-dependent deviations manifest as non-linearities in the carbon budget equation, while scenario-dependent deviations could equally influence both linear and non-linear carbon budget equations. This distinction becomes intuitively evident when viewed through the pulse response lens, where these two effects are independent. In light of the findings in Sect. 4, we can consider two scenarios:
510 one where the model, observed through the pulse response function, exhibits only state-dependent deviations (resulting in a non-linear carbon budget equation), and another where it exclusively displays scenario-dependent deviations while maintaining a linear carbon budget equation. In the case of state-dependent deviations, the pulse response resembles a step function that varies in magnitude with changing climatic conditions. Moreover, as illustrated through the derivation of Eq. (5), if the pulse response (in this case, a step function) decreases in magnitude, the carbon budget equation becomes concave; conversely, if it
515 increases in magnitude, the carbon budget equation becomes convex. On the contrary, for scenarios with scenario-dependency only (without non-linearities), the pulse response must not be a step function. Instead, it needs to exhibit some form of dynamic evolution that eventually leads to the relaxation of the pulse. The example would be the case when the pulse response (e.g., pulse2020) in Fig 1a would not change, thus always retaining the same shape regardless of climatic conditions. In that case the carbon budget equation would be linear (when viewed at the same point) even though it shows scenario-dependent deviations.

520   When it comes to validation of using pulse response as Green's function, the results show that the changing of the pulse under changing background conditions does not affect Green's model's ability to predict scenario dependency to a high degree. By combining these elements, the paper introduces the possibility of approximating the maximum scenario dependency of ESM models. This is achieved by utilizing their pulse response (acting as Green's function) and subjecting it to the optimization program, overcoming computational cost challenges that would otherwise render such an analysis infeasible. This claim
525 remains to be validated in future work in a separate toolset, since the computational costs also prevent the user to validate ESM's Green's function approach the same way it was done in this article.

     When it comes to purely numerical findings in the context of scenario-dependent deviations, it was shown that how much we emit after the optimization year can dramatically affect the generated deviations. For FaIR, the largest possible deviation we acquire is approximately 0.15 K for the transient budget case. In the net-zero case, the largest deviation is well below 0.1
530 K. From the policy-relevant carbon budget viewpoint, this is good news, as it keeps the carbon budget approach resistant to scenario choice while complying with specific temperature targets and net-zero commitments. Regardless of the interpretation, the carbon budget scenario-dependent deviations identified are not permanent but a result of the optimization program in one year. The arguably small deviation diminishes relatively quickly if no further emissions are added to the system. Furthermore, scenario-dependent deviations increase with the higher cumulative emissions cap but do not depend on the optimization

year (supplementary material S2). Moreover, allowing the system to produce negative emissions does not drastically increase scenario-dependent deviations. This shows us that the carbon budget approach is robust to scenario choice in FaIR.

The same conclusion cannot be made for the one-box model. As was shown, the one-box model produces up to 10 times larger scenario-dependent deviations, which evolve in time but do not disappear. The reasons for the dramatically different generated deviations are explained in detail in Sect. 3.2. Besides the one-box model discussed here, the shape comparison of pulse responses presented in Fig. 1 in Dietz et al. (2021) shows that most simple climate models that are being used in climate-economic assessments have some potential for carbon budget scenario dependency – adding weight to the argument for replacing climate emulators with FaIR or any other model whose pulse response shows the right properties, if carbon budget adherence is of importance (presumably, it is).

Moving on, let us consider the connection between the ZEC metric and the pulse response. If ZEC is 0, as the central estimate in MacDougall et al. (2020) suggests, this implies that temperature does not decrease or increase following the cessation of emissions. In the pulse response context, this requires that the pulse response is a step function, or close to it. Plotting the temperature leftover terms (Fig. A1) explicitly shows the FaIR's generated ZEC's under different climatic conditions (i.e., later in RCP run). FaIR initially produces a relatively small negative ZEC ($t_p = 2020$) that actually increases with changing climatic conditions, becoming slightly positive in $t_p = 2100$. This raises the question as to whether ZEC itself is a state-dependent value, i.e., whether the background climatic conditions dictate ZEC's value and to which extent. This question is left to be explored in more advanced models.

Concluding that the carbon budget is indeed unaffected by emission scenario choice confirms the carbon budget approach's value as a tool for directly mapping cumulative emissions to temperature increase. However, the question remains as to the functional form of the carbon budget equation. Sect. 4 provides a method as to how to deduct it from the pulse response representation. Namely, if TCRE is a constant, the carbon budget equation is linear. In Sect. 3, it was shown that the pulse response can be used as a proxy for TCRE, and that the pulse response decreases under changing climatic conditions in the default FaIR parametrization. A method was provided for deriving the non-linear carbon budget deviation from the changing pulse – a general method, which can be used for different models and different model calibrations. This offers an alternative approach to the non-linear carbon budget equation derived in Nicholls et al. (2020), as it does not assume a functional form of the non-linear carbon budget equation in advance, but derives it from TCRE dependency, building on Taylor expansion with respect to temperature, a key thermodynamic variable of the system investigated. As such, the method holds potential to be employed under different parametrizations and different models.

To address the lack of uncertainty in the analysis, Fig. 4 shows different pulse response representations for different FaIR calibrations. Following the methodology explained above, one can deduct that under different parameter sets, FaIR can mimic various levels of carbon budget non-linearity and even full linearity, while keeping scenario-independence robust, as TCRE, which approximates the corresponding pulse responses, can change its magnitude in either direction. This is possible because of the inclusion of both feedbacks on the carbon cycle and the temperature saturation, which counteract each other and can be tuned separately, as mentioned at the beginning of the discussion section. Deriving the carbon budget equation explicitly for each calibration isn't pursued here, as doing so would not yield any new information, and the set is too small to make

570 generalized conclusions on, e.g., how each FaIR parameter affects the (non)linearity of the carbon budget approach. Among other questions raised, this is an interesting aspect for future research.

Finally, the tools used in this paper open a venue to inspect the deviations in other simple models. One promising candidate for developing the research further is the the Model for the Assessment of Greenhouse Gas Induced Climate Change (MAG-ICC), as it provides more detailed information about carbon cycle processes compared to FaIR. (Meinshausen et al., 2011).

575 Given its relative simplicity, MAGICC presents an opportunity to be included in the optimization program, complementing the scenario-independence insights derived from the use of predefined emission scenario sets ((Millar et al., 2016), (Nicholls et al., 2020)). Even without the optimization program, the enhanced resolution of MAGICC in the context of the carbon cycle suggests that examining its pulse response representation under different parametrizations could potentially offer a more comprehensive understanding of the drivers of non-linearities in the carbon budget equation, in comparison to FaIR.

Conclusions

This article focuses on deviations from the carbon budget approach, seen as a linear mapping from cumulative emissions and temperature increase, and draws a clear distinction between carbon budget emission scenario-dependent and climate state-dependent deviation. Scenario-dependent deviations are the possible differences in resulting temperature that are solely due to the preceding emission choice. In contrast, state-dependent deviations underline the change in TCRE value, which depends on

585 the change of background climatic conditions – specifically, the cumulative emissions and global mean temperature increase. Importantly, state-dependent TCRE leads to a non-linear carbon budget equation.

The innovative perspective towards inspecting the carbon budget deviations is provided in the form of inspecting the pulse response representation of a model, i.e., the changing temperature response to an emission pulse (pulse response) under changing climatic conditions. The shape of the pulse response dictates scenario dependency. On the other hand, the change of pulse

590 response with background climatic conditions can be reinterpreted as the state-dependent TCRE, leading to the state-dependent deviations in the form of a non-linear carbon budget equation. The method used to derive the carbon budget equation from pulse response is universal and can be applied under different FaIR calibrations to see how individual climate drivers affect the non-linearity of the carbon budget. This, in combination with employing more complex models' pulse responses as Green's functions, opens a promising avenue for further research.

595 Finally, this article provides an optimization program that tests an entire portfolio of emission scenarios and diagnoses the maximal temperature differences under the same cumulative emissions within the user-defined constraints. As suggested by inspecting its pulse response, FaIR shows small and diminishing deviations compared to the total temperature increase, confirming the carbon budget's robustness when it comes to scenario choice.
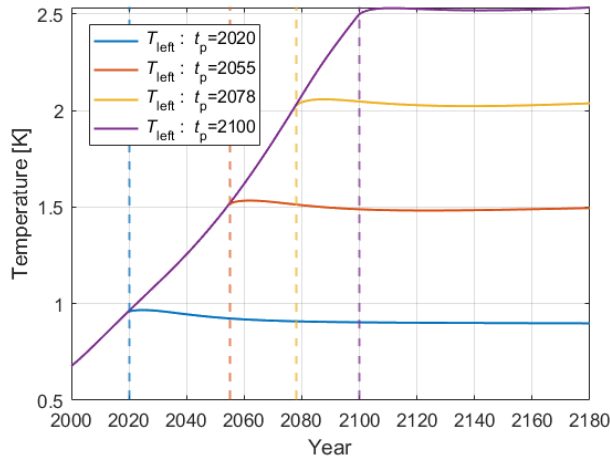
Figure A1. Temperature evolution run up to (RCP6.0 emission scenario) and following the emission cessation at different years t_p. The blue line represents $T_{\text{left}}(t)$, added to Green's integral to compensate for the temperature evolution leftover from prior to the optimization year $t_0 = 2020$.

Appendix A: Temperature leftover in Green's function

When it comes to the magnitudes of $T_{\max}$ and $T_{\min}$, the Green's function approach requires an additional modification to make it comparable with the SCM. If the user is only interested in the deviations, the following modification is not needed. As we can see in Eq. (2), Green's approach responds only to emissions within the integral. That means that in the optimization run, which starts at t_0, it cannot capture the temperature response stemming from emissions predating t_0. Conversely, this is not a problem for the full SCM, since that 'leftover' temperature response is fed into the initial conditions of the run. To overcome this in Green's approach, the 'temperature leftover' parameter $T_{\text{left}}(t)$ to Eq. (2), so it takes the form of $T(t^*) = \int_{t_0}^{t^*} E(\tau) f_{\text{g}}(t^* - \tau) \mathrm{d}\tau + T_{\text{left}}(t^*)$. Notice that the $T_{\text{left}}(t)$ term gets cancelled when the deviation is calculated. The temperature leftover term is generated by feeding FaIR with RCP6.0 emissions until the year t_p, and then setting emissions to zero at the moment of pulse response generation. $T_{\text{left}}(t)$ is assessed as the temperature evolution after emission cessation. Hence, $T_{\text{left}}(t)$ is de facto ZEC by definition. Various temperature leftover values corresponding to different t_p years are shown in Fig. A1. Note that the emission pathways and the years of emission cessation t_p correspond to those of pulse response generation (Fig. 1).

Code and data availability. The codes and data sets used in this analysis can be found online on https://doi.org/10.5281/zenodo.8314808

Competing interests. The author has declared that there are no competing interests.

615 *Acknowledgements.* V. Brovkin pointed out the paper in which the shape of the pulse response function was revealed (Joos et al., 2013). H. Held set this work in motion, as he suggested examining Green's function directly from emissions to temperature and using the minimization and maximization operations to assess scenario dependence. M. Bekchanov provided a GAMS-coded version of FaIR from Bekchanov et al. 'Accuracy of subsidiary climate targets (concentration and cumulative emission) as substitutes to temperature target: trade-offs between overshooting and economic loss' in prep. B. Blanz helped fix and improve the code. I would also like to thank B. Blanz and H. Held for their 620 helpful discussions and careful reading of the manuscript. Finally, I would like to express my sincere and deep gratitude to the anonymous reviewers for their substantial efforts in reading the manuscript and providing constructive criticism, which enabled significant changes and improvements to the manuscript. This research was funded by the Deutsche Forschungsgemeinschaft (DFG, German Research Foundation) under Germany's Excellence Strategy – EXC 2037 'CLICCS - Climate, Climatic Change, and Society' – Project Number: 390683824.

References

Allen, M. R., Frame, D. J., Huntingford, C., Jones, C. D., Lowe, J. A., Meinshausen, M., and Meinshausen, N.: Warming caused by cumulative carbon emissions towards the trillionth tonne, Nature, 458, 1163–1166, publisher: Nature Publishing Group, 2009.

Anthoff, D. and Tol, R. S.: The climate framework for uncertainty, negotiation and distribution (FUND): Technical description, version 3.6, FUND Doc, 2014.

Dietz, S., van der Ploeg, F., Rezai, A., and Venmans, F.: Are Economists Getting Climate Dynamics Right and Does It Matter?, Journal of the Association of Environmental and Resource Economists, 8, 895–921, https://doi.org/10.1086/713977, publisher: The University of Chicago Press, 2021.

Edenhofer, O., Bauer, N., and Kriegler, E.: The impact of technological change on climate protection and welfare: Insights from the model MIND, Ecological Economics, 54, 277–292, https://doi.org/10.1016/j.ecolecon.2004.12.030, 2005.

Forster, P., Storelvmo, T., Armour, K., Collins, W., Dufresne, J.-L., Frame, D., Lunt, D., Mauritsen, T., Palmer, M., Watanabe, M., Wild, M., and Zhang, H.: The Earth's Energy Budget, Climate Feedbacks, and Climate Sensitivity Supplementary Material, in: Climate Change 2021: The Physical Science Basis. Contribution of Working Group I to the Sixth Assessment Report of the Intergovernmental Panel on Climate Change, edited by Masson-Delmotte, V., Zhai, P., Pirani, A., Connors, S. L., Péan, C., Berger, S., Caud, N., Chen, Y., Goldfarb, L., Gomis, M. I., Huang, M., Leitzell, K., Lonnoy, E., Matthews, J. B. R., Maycock, T. K., Waterfield, T., Yelekçi, O., Yu, R., and Zhou, B., book section 7, Cambridge University Press, Cambridge, UK and New York, NY, USA, https://www.ipcc.ch/report/ar6/wg1/downloads/report/IPCC_AR6_WGI_Chapter07_SM.pdf, 2021.

Gillett, N. P., Arora, V. K., Matthews, D., and Allen, M. R.: Constraining the Ratio of Global Warming to Cumulative CO_2 Emissions Using CMIP5 Simulations, Journal of Climate, 26, 6844–6858, https://doi.org/10.1175/JCLI-D-12-00476.1, publisher: American Meteorological Society Section: Journal of Climate, 2013.

Hajima, T., Watanabe, M., Yamamoto, A., Tatebe, H., Noguchi, M. A., Abe, M., Ohgaito, R., Ito, A., Yamazaki, D., Okajima, H., et al.: Development of the MIROC-ES2L Earth system model and the evaluation of biogeochemical processes and feedbacks, Geoscientific Model Development, 13, 2197–2244, 2020.

Herrington, T. and Zickfeld, K.: Path independence of climate and carbon cycle response over a broad range of cumulative carbon emissions, Earth System Dynamics, 5, 409–422, 2014.

Hope, C.: The marginal impact of CO_2 from PAGE2002: an integrated assessment model incorporating the IPCC's five reasons for concern, Integrated Assessment Journal, 6, 2006.

Joos, F., Roth, R., Fuglestvedt, J. S., Peters, G. P., Enting, I. G., Von Bloh, W., Brovkin, V., Burke, E. J., Eby, M., Edwards, N. R., et al.: Carbon dioxide and climate impulse response functions for the computation of greenhouse gas metrics: a multi-model analysis, Atmospheric Chemistry and Physics, 13, 2793–2825, 2013.

Khabbazan, M. M. and Held, H.: On the future role of the most parsimonious climate module in integrated assessment, Earth System Dynamics, 10, 135–155, 2019.

Lahn, B.: A history of the global carbon budget, WIREs Climate Change, 11, e636, https://doi.org/10.1002/wcc.636, _eprint: https://onlinelibrary.wiley.com/doi/pdf/10.1002/wcc.636, 2020.

Leach, N. J., Jenkins, S., Nicholls, Z., Smith, C. J., Lynch, J., Cain, M., Walsh, T., Wu, B., Tsutsui, J., and Allen, M. R.: FaIRv2.0.0: a generalized impulse response model for climate uncertainty and future scenario exploration, Geoscientific Model Development, 14, 3007–3036, https://doi.org/10.5194/gmd-14-3007-2021, publisher: Copernicus GmbH, 2021.

Leduc, M., Matthews, H. D., and Elía, R. d.: Quantifying the Limits of a Linear Temperature Response to Cumulative CO2 Emissions, Journal of Climate, 28, 9955–9968, https://doi.org/10.1175/JCLI-D-14-00500.1, publisher: American Meteorological Society Section: Journal of Climate, 2015.

MacDougall, A. H.: The oceanic origin of path-independent carbon budgets, Scientific Reports, 7, 10 373, 2017.

665 MacDougall, A. H. and Friedlingstein, P.: The origin and limits of the near proportionality between climate warming and cumulative CO2 emissions, Journal of Climate, 28, 4217–4230, 2015.

MacDougall, A. H., Frölicher, T. L., Jones, C. D., Rogelj, J., Matthews, H. D., Zickfeld, K., Arora, V. K., Barrett, N. J., Brovkin, V., Burger, F. A., et al.: Is there warming in the pipeline? A multi-model analysis of the Zero Emissions Commitment from CO 2, Biogeosciences, 17, 2987–3016, 2020.

670 Masson-Delmotte, V., Zhai, P., Pirani, A., Connors, S. L., Péan, C., Berger, S., Caud, N., Chen, Y., Goldfarb, L., Gomis, M. I., Huang, M., Leitzell, K., Lonnoy, E., Matthews, J. B. R., Maycock, T. K., Waterfield, T., Yelekçi, O., Yu, R., and Zhou, B., eds.: Summary for policymakers, pp. 3–32, Cambridge University Press, https://doi.org/10.1017/9781009157896.001, 2021.

Matthews, H. D. and Weaver, A. J.: Committed climate warming, Nature Geoscience, 3, 142–143, 2010.

Matthews, H. D., Gillett, N. P., Stott, P. A., and Zickfeld, K.: The proportionality of global warming to cumulative carbon emissions, Nature,
675 459, 829–832, https://doi.org/10.1038/nature08047, number: 7248 Publisher: Nature Publishing Group, 2009.

Meinshausen, M., Meinshausen, N., Hare, W., Raper, S. C. B., Frieler, K., Knutti, R., Frame, D. J., and Allen, M. R.: Greenhouse-gas emission targets for limiting global warming to 2 °C, Nature, 458, 1158–1162, https://doi.org/10.1038/nature08017, number: 7242 Publisher: Nature Publishing Group, 2009.

Meinshausen, M., Raper, S. C., and Wigley, T. M.: Emulating coupled atmosphere-ocean and carbon cycle models with a simpler model,
680 MAGICC6–Part 1: Model description and calibration, Atmospheric Chemistry and Physics, 11, 1417–1456, 2011.

Millar, R., Allen, M., Rogelj, J., and Friedlingstein, P.: The cumulative carbon budget and its implications, Oxford Review of Economic Policy, 32, 323–342, https://doi.org/10.1093/oxrep/grw009, 2016.

Millar, R. J., Nicholls, Z. R., Friedlingstein, P., and Allen, M. R.: A modified impulse-response representation of the global near-surface air temperature and atmospheric concentration response to carbon dioxide emissions, Atmospheric Chemistry and Physics, 17, 7213–7228,
685 https://doi.org/10.5194/acp-17-7213-2017, publisher: Copernicus GmbH, 2017.

Müller, W. A., Jungclaus, J. H., Mauritsen, T., Baehr, J., Bittner, M., Budich, R., Bunzel, F., Esch, M., Ghosh, R., Haak, H., et al.: A higher-resolution version of the max planck institute earth system model (MPI-ESM1. 2-HR), Journal of Advances in Modeling Earth Systems, 10, 1383–1413, 2018.

Nicholls, Z.: Reduced Complexity Model Intercomparison Project (RCMIP), pp. EGU21–3707, https://doi.org/10.5194/egusphere-egu21-
690 3707, conference Name: EGU General Assembly Conference Abstracts ADS Bibcode: 2021EGUGA..23.3707N, 2021.

Nicholls, Z., Gieseke, R., Lewis, J., Nauels, A., and Meinshausen, M.: Implications of non-linearities between cumulative CO2 emissions and CO2-induced warming for assessing the remaining carbon budget, Environmental Research Letters, 15, 074 017, 2020.

Petschel-Held, G., Schellnhuber, H.-J., Bruckner, T., Toth, F. L., and Hasselmann, K.: The tolerable windows approach: theoretical and methodological foundations, Climatic Change, 41, 303–331, 1999.

695 Raupach, M. R.: The exponential eigenmodes of the carbon-climate system, and their implications for ratios of responses to forcings, Earth System Dynamics, 4, 31–49, https://doi.org/10.5194/esd-4-31-2013, 2013.

Ricke, K. L. and Caldeira, K.: Maximum warming occurs about one decade after a carbon dioxide emission, Environmental Research Letters, 9, 124 002, 2014.

Rogelj, J., Shindell, D., Jiang, K., Fifita, S., Forster, P., Ginzburg, V., Handa, C., Kheshgi, H., Kobayashi, S., Kriegler, E., et al.: Mitigation
pathways compatible with 1.5 C in the context of sustainable development, in: Global warming of 1.5 C, pp. 93–174, Intergovernmental
Panel on Climate Change, 2018.

Séférian, R., Nabat, P., Michou, M., Saint-Martin, D., Voldoire, A., Colin, J., Decharme, B., Delire, C., Berthet, S., Chevallier, M., et al.:
Evaluation of CNRM Earth System Model, CNRM-ESM2-1: Role of Earth system processes in present-day and future climate, Journal
of Advances in Modeling Earth Systems, 11, 4182–4227, 2019.

Shine, K. P., Fuglestvedt, J. S., Hailemariam, K., and Stuber, N.: Alternatives to the global warming potential for comparing climate impacts
of emissions of greenhouse gases, Climatic change, 68, 281–302, 2005.

Stocker, T. F., Qin, D., Plattner, G.-K., Tignor, M., Allen, S. K., Doschung, J., Nauels, A., Xia, Y., Bex, V., and Midgley, P. M., eds.: Summary
for policymakers, pp. 3–29, Cambridge University Press, Cambridge, UK, https://doi.org/10.1017/CBO9781107415324.004, 2013.

Wu, T., Lu, Y., Fang, Y., Xin, X., Li, L., Li, W., Jie, W., Zhang, J., Liu, Y., Zhang, L., et al.: The Beijing Climate Center climate system model
(BCC-CSM): The main progress from CMIP5 to CMIP6, Geoscientific Model Development, 12, 1573–1600, 2019.

Zickfeld, K., Eby, M., Matthews, H. D., and Weaver, A. J.: Setting cumulative emissions targets to reduce the risk of dangerous climate
change, Proceedings of the National Academy of Sciences, 106, 16 129–16 134, https://doi.org/10.1073/pnas.0805800106, publisher:
Proceedings of the National Academy of Sciences, 2009.

Ziehn, T., Chamberlain, M. A., Law, R. M., Lenton, A., Bodman, R. W., Dix, M., Stevens, L., Wang, Y.-P., and Srbinovsky, J.: The Australian
earth system model: ACCESS-ESM1. 5, Journal of Southern Hemisphere Earth Systems Science, 70, 193–214, 2020.